研究論文

Structures and Photocatalytic Performance of TiO_2-$FeTiO_3$ Coatings Prepared by Plasma Spraying Technique

Fuxing YE*, Akira OHMORI***, Kazuhiro NAKATA** and Takuya TSUMURA**

(Received August 21, 2007)

$FeTiO_3$ with band gap of 2.85 eV was added into TiO_2 powder to improve the visible light responsivity of TiO_2 in this study. The compositions and photocatalytic activity of plasma sprayed TiO_2, TiO_2-30%$FeTiO_3$, TiO_2-50%$FeTiO_3$ and $FeTiO_3$ coatings were investigated. The influence of $FeTiO_3$ compound on the charge carrier separation and recombination in the TiO_2-$FeTiO_3$ coating was discussed. The $FeTiO_3$ coating plasma sprayed under the arc current of 400 A consisted of rutile TiO_2, $FeTiO_3$, Fe_2TiO_5, and thermally metastable $Fe_2Ti_3O_9$ and γ-Fe_2O_3. TiO_2-30%$FeTiO_3$ coating sprayed under the arc current of 400 A, which contained anatase TiO_2, rutile TiO_2 and $FeTiO_3$, had good photocatalytic activity. The relative deposition rate of TiO_2-30%$FeTiO_3$ powder under the arc current of 400 A was approximate to 4 μm/pass. For the low band gap of pure $FeTiO_3$ compound, the existence of $FeTiO_3$ could improve the photocatalytic activity of anatase TiO_2 when $FeTiO_3$ contacts coherently with it, which was explained using a proposed two-steps electron transfer model.

Key Words: TiO_2, plasma spray, photocatalyst, $FeTiO_3$

1. Introduction

To solve the environmental problems related to the hazardous wastes, contaminated groundwater and toxic air contaminants, extensive research is underway to develop commercial photocatalysts, which include TiO_2, CdS, SnO_2, WO_3, SiO_2, ZrO_2, ZnO, Nb_2O_5, Fe_2O_3, $SrTiO_3$ etc[1-11]. Among all the oxide semiconductors that have been reported, titanium dioxide is an excellent photocatalyst due to its optical and electronic properties, chemical stability, non-toxicity and low cost[12-17].

However, it has been also realized that the band gap of anatase TiO_2 (about 3.2 eV) means that the electron can only be excited from the valence to the conduction band by the high power light irradiation with a wavelength less than 387 nm. This limits the application of sunlight as an energy source for the photocatalysis. Recently, visible light responsive photocatalysts are studied intensively. For example, Anpo have synthesized iron-ion-doped anatase TiO_2 by the hydrothermal method from Titanium (IV) tetra-tert-butoxide and $FeCl_3$ or $FeCl_2$ solution[18]. The amount of doped iron ion plays a significant role in affecting its photocatalytic activity and iron doped with optimum content can enhance photocatalytic activity, especially under visible light irradiation. Anpo also reported that the Fe ion-implanted TiO_2 catalysts enable the absorption of visible light up to a wavelength of 400-600 nm[19].

The trigonal crystal $FeTiO_3$ is widespread in nature, and it is found as a fundamental component of ilmenite and as one of the main materials showing remnant magnetic properties. The structure of $FeTiO_3$ is derived from that of α-Fe_2O_3 by replacing every other layer of Fe atoms in (0001) planes by a layer of Ti atoms[20, 21]. The band gap of bulk $FeTiO_3$ is 2.85 eV[22], which means it can absorb visible light. Ilmenite is an incongruent melting material with the melting point of approximately 1683K[23]. Although high temperature electrical conductivity and magnetic properties of ilmenite $FeTiO_3$ have been investigated in detail[20-25], very little work has been done as a chemical catalyst and photocatalyst[26]. The characterization of photocatalytic performance of TiO_2-$FeTiO_3$ composite cannot be found until now.

Recently, plasma spraying technique is widely applied to fabricate coating using feedstock powders such as ZrO_2, Al_2O_3 and TiO_2 to improve surface wear resistance. The coating formation speed is very high and it is easy to form composite coatings. A plasma sprayed coating is formed by a stream of molten or half molten droplets impacting on the substrate followed by flattening, rapid solidification, and cooling processes. The individual molten droplets spread to thin lamellae, the stacking of which constitutes the coating[27]. In this study, plasma

* School of Materials Science & Engineering, Tianjin University (Weijin Road No.92, Tianjin, 300072, P.R.China)
** Joining and Welding Research Institute, Osaka University (11-1 Mihogaoka, Ibaraki, Osaka 567-0047 Japan)
*** TOCALO Co. Ltd. (Minamifutami, Futami-Cho, Akashi, Hyogo 674-0093 Japan)

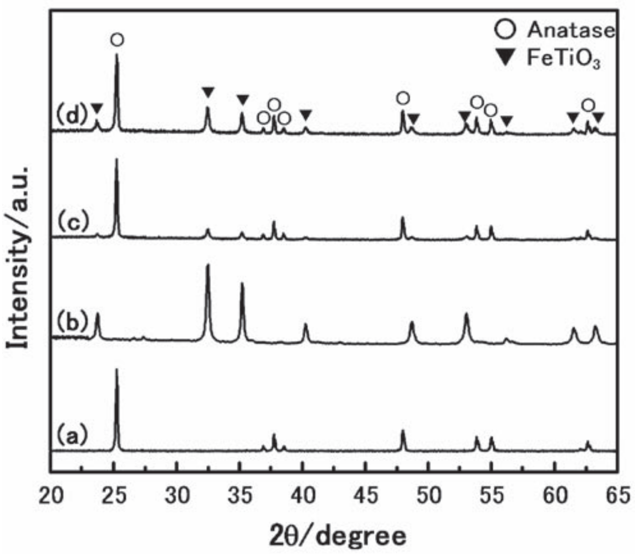

Fig.1. X-ray diffraction patterns of the TiO_2 (a), $FeTiO_3$ (b), TiO_2-30%$FeTiO_3$ (c) and TiO_2-50%$FeTiO_3$ (d) feedstock powders.

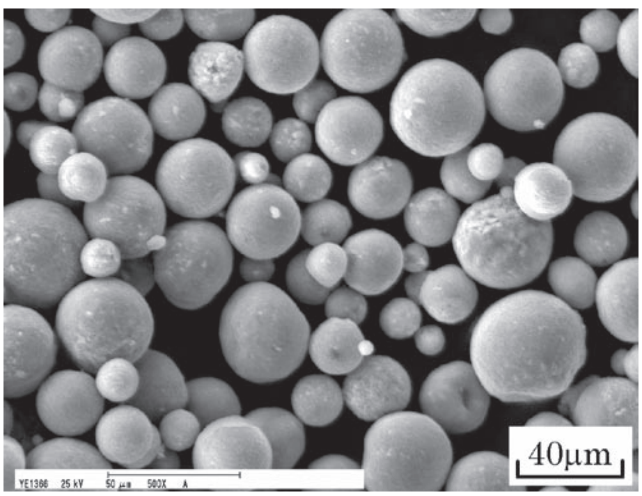

Fig.2. The morphology of TiO_2-30%$FeTiO_3$ powder.

spraying technique was applied to deposit photocatalytic coating.

To elucidate the influence of $FeTiO_3$ on the photocatalytic activity of plasma sprayed TiO_2-$FeTiO_3$ coatings, TiO_2, $FeTiO_3$ and TiO_2-$FeTiO_3$ powders were designed in this study. The phase composition, microstructure and photocatalytic activity of plasma sprayed $FeTiO_3$, TiO_2-30%$FeTiO_3$ and TiO_2-50%$FeTiO_3$ coatings were discussed in detail.

2. Materials and experimental procedure

2.1 Feedstock powders and substrate

$FeTiO_3$ particles with average size of 1.4 μm were agglomerated to $FeTiO_3$ feedstock powder with average size of 32.5 μm. To manufacture TiO_2-30%$FeTiO_3$ and TiO_2-50%$FeTiO_3$ feedstock powders, TiO_2 particle with average size of 0.2 μm was mechanically and uniformly mixed with 1.4 μm $FeTiO_3$ particles with corresponding weight ratio. The average size of TiO_2, TiO_2-30%$FeTiO_3$ and TiO_2-50%$FeTiO_3$ feedstock powders was 33.7 μm, 30.4 μm and 28.9 μm, respectively. The x-ray diffraction patterns of the TiO_2, $FeTiO_3$, TiO_2-30%$FeTiO_3$ and TiO_2-50%$FeTiO_3$ feedstock powders are shown in **Fig.1**. The morphology of TiO_2-30%$FeTiO_3$ powder was spheric as given in **Fig.2**, and it was very similar to TiO_2, $FeTiO_3$ and TiO_2-50%$FeTiO_3$ powder. The substrate was stainless steel (JIS SUS304), which was washed by acetone and sandblasted before thermal spray. The dimensions of the substrate were 50 × 60 × 3 mm.

Table1 Plasma spraying parameters.

Argon gas pressure (MPa) /flow (slpm)	0.42/58
Helium gas pressure (MPa) /flow (slpm)	0.21/9
Arc current (A)	400, 600, 800
Arc voltage (V)	28~30
Spraying distance (mm)	70

2.2 Plasma spraying equipment

The thermal spraying equipment was a plasma spraying system (Plasmadyne-Mach1, Miller Thermal, USA). Argon was applied as primary gas, and helium was applied as secondary gas. The powder was fed from the inner hole of the anode. The thermal spraying parameters are given in **Table 1**.

2.3 Characterization of powders and sprayed coatings

Electron probe surface roughness analyzer (ERA-8800FE, Elionix Co. Ltd., Japan) and energy dispersive analysis of x-ray (EDAX) were used to examine the structure characteristics of the feedstock powders and the sprayed coatings. The phase composition of the feedstock powders and the sprayed coatings was investigated by x-ray diffraction using Cu-Kα radiation (λ =1.5406 Å) and graphite crystal monochromator (M03XHF, MAC Science Co. Ltd.).

In this experiment, the photocatalytic activity of the sprayed coatings was evaluated through the photo decomposition of acetaldehyde. The ultraviolet light (peak wavelength was 352 nm) intensity on the sample surface was set in 1.0 mW/cm^2. In the experimental procedure, the concentration (ppm) of the foul gas with time (s) was measured with a Kitakawa type gas detector at a certain time interval.

The reported results for photocatalytic efficiency of titanium dioxide indicated that the destruction rates of various contaminants by photocatalyst fit the Langmuir-Hinshelwood kinetic equation[28, 29]. Langmuir-Hinshelwood explains the kinetics of heterogeneous catalytic processes and Langmuir adsorption isotherm is valid for the surface reaction. It is a first order kinetic equation. The Langmuir-Hinshelwood rate form is

$$\ln\left(\frac{C_0}{C}\right) = t / \tau \qquad (1)$$

where C is the concentration of the reactant (ppm), C_0 the initial concentration of the reactant (ppm), t the irradiation time (s), τ the constant of photocatalytic activity. According to equation (1), the smaller of the τ value the better of the photocatalytic activity of the coating.

2.4 Definition of relative deposition rate of feedstock powder

In thermal spray technology, many parameters are applied to evaluate the properties of sprayed coatings, such as cohesion strength, hardness, wear resistance, powder deposition efficiency and so on. The mechanical properties of sprayed coatings are very important in mechanical applications. However, great attention should be paid on not only the functional performance but also the powder deposition rate in the developments of functional coatings.

Therefore, to evaluate the fabrication characteristics of the feedstock powder at various plasma spraying conditions, the powder deposition rate was defined as Equation (2). The calculated result was applied to compare the powder deposition efficiency in this study.

$$RDRP = \frac{T_{Thickness} V_{Traverse} W_{Step}}{n V_{Rotation}} \qquad (2)$$

where RDRP is Relative Deposition Rate of Powder, $V_{Rotation}$ relative rotation speed of powder feeder, $V_{Traverse}$ relative traverse speed of plasma gun, W_{Step} relative step width of up-down moving equipment, $T_{Thickness}$ thickness of sprayed coating, n spray pass of the coating.

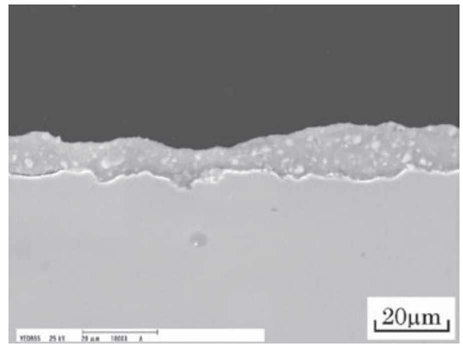

(a)

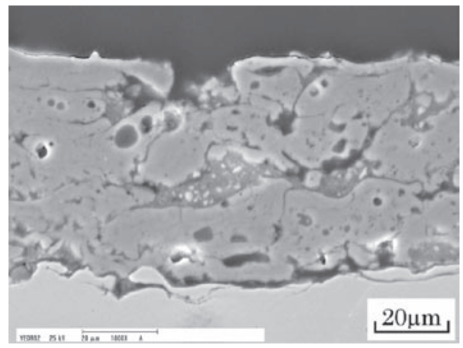

(b)

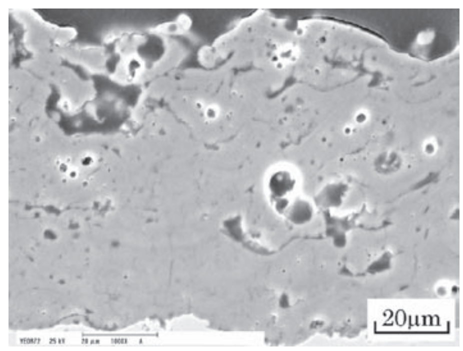

(c)

Fig.3. Cross sections of TiO_2-30%$FeTiO_3$ coatings sprayed under the arc current of 400 A(a), 600 A(b) and 800 A(c).

3. Results and discussion

3.1 Typical microstructure of $FeTiO_3$ and TiO_2-$FeTiO_3$ coatings

Figure 3 shows the effect of the arc current on the microstructure of TiO_2-30%$FeTiO_3$ sprayed coatings. It indicates that the coating became denser with the increasing of arc current for the higher plasma power. As clearly shown in **Fig.4**, many primary particles with average size of about 200 nm remained in the coating sprayed under the arc current of 400 A for the low energy transferred from plasma jet. The relative deposition rate of TiO_2-30%$FeTiO_3$ powder, which was approximate to 4 μm/pass, did not differ significantly from that of TiO_2 powder as shown in **Fig. 5**. With the increase of arc current to 600 A or 800 A, the relative deposition rate of TiO_2-30%$FeTiO_3$ powder (RDRP) increased obviously.

3.2 Compositions of $FeTiO_3$ and TiO_2-$FeTiO_3$ coatings

The x-ray diffraction pattern of plasma sprayed $FeTiO_3$ coating under the arc current of 400 A is illustrated in **Fig.6**(a). The $FeTiO_3$ coating consisted of rutile TiO_2, $FeTiO_3$, Fe_2TiO_5, $Fe_2Ti_3O_9$ and γ-Fe_2O_3 (maghemite). Y. Chen et al.[30, 31] reported that the thermal oxidation process of $FeTiO_3$ by high energy ball milling in air consists reactions (3)~(5). The $Fe_2Ti_3O_9$ and γ

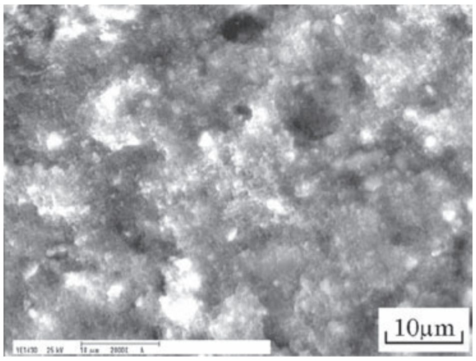

(a)

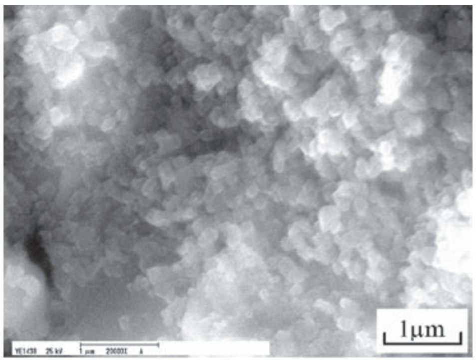

(b)

Fig.4. Surface morphologies of TiO_2-30%$FeTiO_3$ coating sprayed under the arc current of 400A ((a) low magnification, (b) high magnification.).

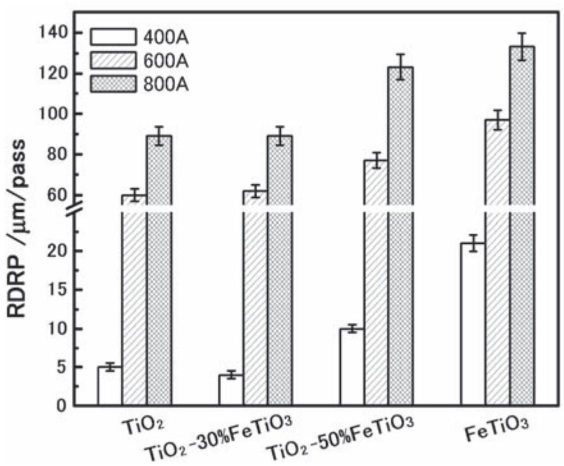

Fig.5. Relative deposition rate of TiO_2, TiO_2-30%$FeTiO_3$, TiO_2-50%$FeTiO_3$ and $FeTiO_3$ powder (RDRP) under the arc current of 400 A, 600 A and 800 A.

-Fe_2O_3 are thermally metastable products which are normally difficult or impossible to be produced by conventional thermal equilibrium processes. These metastable phases were also observed in plasma sprayed $FeTiO_3$ coatings. Thus it can also be inferred that plasma spraying technique is a method to form metastable substance.

$$4FeTiO_3 + O_2 \rightarrow Fe_2Ti_3O_9 + TiO_2 + Fe_2O_3 \quad (3)$$

$$Fe_2O_3 + TiO_2 \rightarrow Fe_2TiO_5 \quad (4)$$

$$Fe_2Ti_3O_9 \rightarrow Fe_2TiO_5 + 2TiO_2 \quad (5)$$

The TiO_2-30%$FeTiO_3$ coating sprayed under the arc current of 400 A consisted of anatase TiO_2, rutile TiO_2 and $FeTiO_3$ as illustrated in **Fig. 6**(b). Under the arc current of 400 A, large part of anatase TiO_2 and $FeTiO_3$ still remained in it, and Fe_2TiO_5 and $Fe_2Ti_3O_9$ phase were undetectable. With the increasing of arc current to 600 A or 800 A, Fe_2TiO_5, $Fe_2Ti_3O_9$ and Fe_2O_3 phases appeared in the sprayed TiO_2-30%$FeTiO_3$ coatings.

As illustrated in **Fig. 6**(c), with the increase of the weight content of $FeTiO_3$ from 30% to 50% in the TiO_2-$FeTiO_3$ feedstock powder, $Fe_2Ti_3O_9$ and Fe_2TiO_5 phases appeared under the low arc current of 400 A for the large content of $FeTiO_3$ in the powder.

3.3 Photocatalytic activity of $FeTiO_3$ and TiO_2-$FeTiO_3$ coatings

Figure 7 shows the τ values of plasma sprayed TiO_2, TiO_2-30%$FeTiO_3$, TiO_2-50%$FeTiO_3$ and $FeTiO_3$ coatings under the arc current of 400A and 600A. The results revealed that the photocatalytic activity of TiO_2-30%$FeTiO_3$ coating was better than that of the other three coatings plasma sprayed under the same arc current. As mentioned above, the TiO_2-30%$FeTiO_3$ coating sprayed under the arc current of 400 A consisted of TiO_2 and $FeTiO_3$ only. The band gap of bulk $FeTiO_3$, which is 2.85 eV[26)], is lower than that of TiO_2. Scaife[32)] summarized the findings of some oxide semiconductors including $FeTiO_3$ on the flat band potential, band gaps and stabilities, and the findings indicate the valence band edge of $FeTiO_3$ is about in the same level with that of TiO_2. Therefore, as a possible phenomenon shown in **Fig. 8**, when the semiconductor was irradiated, the electron possibly transferred (moved) to conduction band in two steps in composite TiO_2-$FeTiO_3$. First step: the electron was initiated from the valence band to the conduction band of TiO_2, and second step: the electron in the conduction band of TiO_2 injected to the conduction band of $FeTiO_3$. For this two-steps mechanism, the lifetime of excited hole and electron pair was prolonged. Perhaps the improved efficiency of the photon was a reason for the good photocatalytic activity of the TiO_2-30%$FeTiO_3$ coating sprayed under the arc current of 400 A.

It was reported that the recombination rate of the excited electron-hole in the rutile TiO_2 and Fe_2TiO_5 is higher than that in anatase TiO_2[33)]. As for the sprayed TiO_2-50%$FeTiO_3$ coatings, the

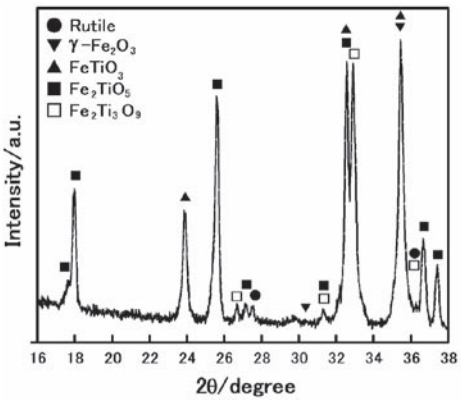

(a)

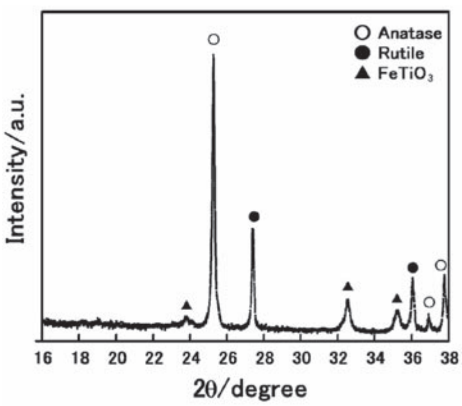

(b)

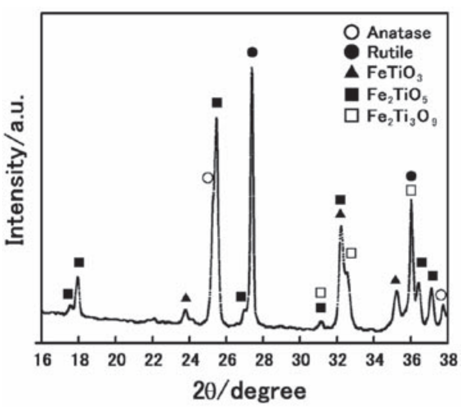

(c)

Fig.6. X-ray diffraction patterns of $FeTiO_3$ (a), TiO_2-30%$FeTiO_3$ (b) and TiO_2-50%$FeTiO_3$ (c) coatings plasma sprayed under the arc current of 400A and spraying distance of 70 mm.

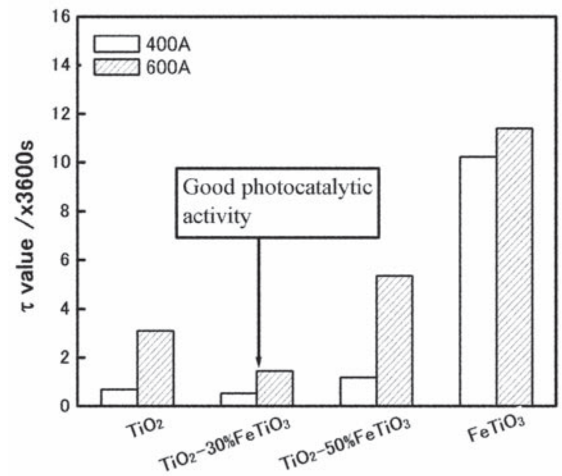

Fig.7. τ values of plasma sprayed TiO_2, TiO_2-30%$FeTiO_3$, TiO_2-50%$FeTiO_3$ and $FeTiO_3$ coatings under the arc current of 400A and 600A.

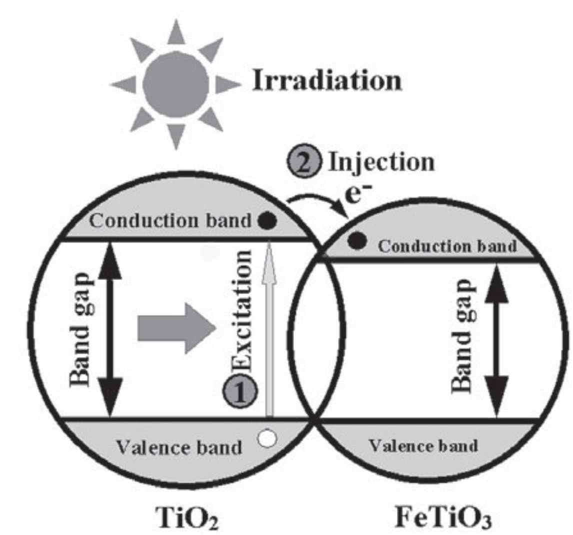

Fig.8. A proposed two-steps electron transfer model for the good photocatalytic activity of TiO_2-30%$FeTiO_3$ coating.

anatase content of TiO_2 was very low and the content of Fe_2TiO_5 was very high for the more addition of $FeTiO_3$. This resulted in the low photocatalytic activity of the TiO_2-50%$FeTiO_3$ coatings comparing to that of the sprayed TiO_2-30%$FeTiO_3$ coating

As a result, the compositions of the sprayed coatings had great influence on the photocatalytic activity. For the low band gap of pure $FeTiO_3$ compound, the existence of $FeTiO_3$ could improve the photocatalytic activity of anatase TiO_2 when $FeTiO_3$ contacts coherently with it.

4. Conclusions

To improve the visible light responsibility of TiO_2, $FeTiO_3$ with band gap of 2.85eV was added into TiO_2 powder to fabricate high photocatalytic coating by plasma spraying technique. The compositions and photocatalytic activity of plasma sprayed $FeTiO_3$, TiO_2-30%$FeTiO_3$ and TiO_2-50%$FeTiO_3$ coatings were investigated. The influence of $FeTiO_3$ compound on the charge carrier separation and recombination in the TiO_2-$FeTiO_3$ coating was discussed. The $FeTiO_3$ coating plasma sprayed under the arc current of 400 A consisted of rutile TiO_2, $FeTiO_3$, Fe_2TiO_5, and thermally metastable $Fe_2Ti_3O_9$ and γ-Fe_2O_3. TiO_2-30%$FeTiO_3$ coating sprayed under the arc current of 400 A, which contained anatase TiO_2, rutile TiO_2 and $FeTiO_3$, had good photocatalytic character because the coating did not contain the unfavorable Fe_2TiO_5 phase. A two-steps electron transfer model was proposed to explain this character according to the level of valence band edge and band gap of the two substances of $FeTiO_3$ and TiO_2. The relative deposition rate of TiO_2-30%$FeTiO_3$ powder under the arc current of 400 A was approximate to 4 μm/pass.

Acknowledgment

This work was supported by the Scientific Research Foundation for the Returned Overseas Chinese Scholars, Tianjin.

References

1) A. Fujishima, K. Honda: Nature, 238 (1972) 37-38.
2) A. Fujishima, T. N. Rao, D. A. Tryk: J. Photoch. Photobio. C: Photoch. Rev., 1 (2000) 1-21.
3) J. A. Navío, G. Colón, M. Macías, P. J. Sánchez-Soto, V. Augugliaro and L. Palmisano: J. Mol. Catal. A-Chem., 109 (1996) 239-248.
4) J.A. Navio, G. Colon, J.M. Herrmann: J. Photoch. Photobio. A, 108 (1997) 179-185.
5) L. Bahadur, N.R. Tata: J. Photoch. Photobio. A, 91 (1995) 233-240.
6) M.R. Dhananjeyan, V. Kandavelu, R. Renganathan: J. Mol. Catal. A-Chem., 151 (2000) 217-223.
7) B. Pal, T. Hata, K. Goto, G. Nogami: J. Mol. Catal. A-Chem., 169 (2001) 147-155.
8) A.K.G. Carlos, F. Wypych, S.G. Moraes, N. Duran, N. Nagata, P. Peralta-Zamora: Chemosphere, 40 (2000) 433-440.
9) B. Neppolian, H. C. Choi, S. Sakthivel, Banumathi Arabindoo and V. Murugesan: J. Harz. Mater., 89 (2002) 303-317.
10) L. Bayer, I. Eroglu, L. Turker: Sol. Energ. Mat. Sol. C., 62 (2000) 43-49.
11) F. X. Ye and A. Ohmori: Surf. Coat. Technol., 160 (2002) 62-67.
12) P. Calza, C. Minero, A. Hiskia: Appl. Catal. B-Environ., 21-3 (1999) 191-202.
13) A. Mills, J. Wang: J. Photoch. Photobio. A, 127 (1999) 123-134.
14) K. Tennakone, U.S. Ketipearachchi: Appl. Catal. B-Environ., 5 (1995) 343-349.
15) F. Zhang, J. Zhao, T. Shen, H. Hidaka, E. Pelizzetti, N. Serpone: Appl. Catal. B-Environ., 15 (1998) 147-156.
16) A. Sclafani, J. Herrmann: J. Photoch. Photobio. A, 113-2 (1998) 181-188.
17) Ilisz, Z. Laszlo, A. Dombi: Appl. Catal. A-Gen., 180 (1999) 25-33.
18) J.-F Zhu, W. Zheng, B. He, J.-L Zhang, M. Anpo: J. Mol. Cata. A: Chem., 216 (2004) 35-43.
19) H. Yamashita, M. Harada, J. Misaka, M. Takeuchi, B. Neppolian, and M. Anpo: Cata. Today, 84 (2003) 191-196.
20) R. W. Taylor: Am. Mineral., 49 (1964) 1016-1030.
21) Y. Ishikawa and S. Akimoto: J. Phys. Soc. Jpn., 12-10 (1957) 1083-1098.
22) M. A. Butler and D. S. Ginley: Chem. Phys. Lett., 47-2 (1977) 319-321.
23) F. Zhou, S. Kotru, and R. K. Pandey: Thin Solid Films, 408 (2002) 33-36.
24) P. F. McMonald, A. Parasiris, R. K. Pandey, B. L. Gries, and W. P. Kirk: J. Appl. Phys., 69-2, (1991) 1104-1106.
25) Y. Ishikawa and S. Sawada: J. Phys. Soc. Jpn., 11-5 (1956) 496-835.
26) Y. Ishikawa and S. Akimoto: J. Phys. Soc. Jpn., 13-10 (1958) 1110-1118.
27) C.-J. Li and A. Ohmori: J. Therm. Spray Technol., 11 (2002) 365-374.
28) A.V. Vorontsov, A.A. Altynnikov: J. Photochem. Photobiol., A 144 (2001) 193-196.
29) P.H. Chen, C.H. Jen:Q Environ. Int., 24-8 (1998) 871-879.
30) Y. Chen: J. Alloy. Comp., 257 (1997) 156-160.
31) Y. Chen: J. Alloy. Comp., 266 (1998) 150-154.
32) D.E. Scaife: Solar Energy, 25 (1980) 41-54.
33）B. Pal, M. Sharon, and G. Nogami: Mater. Chem. and Phys., 9-3 (1999) 254-261.